Bioactive Materials 3 (2018) 167–173

Contents lists available at ScienceDirect

Bioactive Materials

journal homepage: http://www.keaipublishing.com/en/journals/bioactive-materials/

Bioactive polydimethylsiloxane surface for optimal human mesenchymal stem cell sheet culture

Zichen Qian, David Ross, Wenkai Jia, Qi Xing, Feng Zhao*

Department of Biomedical Engineering, Michigan Technological University, 1400 Townsend Drive, Houghton, MI 49931, USA

ARTICLE INFO

Article history:
Received 20 November 2017
Received in revised form
22 January 2018
Accepted 26 January 2018

Keywords:
Cell sheet engineering
Human mesenchymal stem cell
Polydimethylsiloxane
Layer-by-layer grafting
Cell adhesion

ABSTRACT

Human mesenchymal stem cell (hMSC) sheets hold great potential in engineering three-dimensional (3D) completely biological tissues for diverse applications. Conventional cell sheet culturing methods employing thermoresponsive surfaces are cost ineffective, and rely heavily on available facilities. In this study, a cost-effective method of layer-by-layer grafting was utilized for covalently binding a homogenous collagen I layer on a commonly used polydimethylsiloxane (PDMS) substrate surface in order to improve its cell adhesion as well as the uniformity of the resulting hMSC cell sheet. Results showed that a homogenous collagen I layer was obtained via this grafting method, which improved hMSC adhesion and attachment through reliable collagen I binding sites. By utilizing this low-cost method, a uniform hMSC sheet was generated. This technology potentially allows for mass production of hMSC sheets to fulfill the demand of thick hMSC constructs for tissue engineering and biomanufacturing applications.

1. Introduction

Creating suitable materials for tissue engineering is challenging due to the lack of bioactivity and biocompatibility for most synthetic materials [1]. Scaffold-free tissue engineering constructs have gained popularity because they eliminate the potential release of regeneration discouraging molecules from the scaffold [2]. Pioneered by Okano group, cell sheet engineering is an effective technology to create cell-dense constructs with preserved extracellular matrix (ECM) contents [3]. Those ECM biomacromolecules are bioactive, and can be tailored to have unique properties by employing specific cell types [4,5].

Human mesenchymal stem cells (hMSCs) can be easily obtained from bone marrow, adipose tissues, and peripheral blood. They can also be extensively expanded *in vitro* to fulfill substantial demand [6]. Moreover, hMSCs are multi-potent, immune-modulatory, and regenerative [7]. These unique properties make hMSC sheets especially attractive in engineering three-dimensional (3D) completely biological tissues for diverse applications. Our previous studies have demonstrated that hMSC sheets can be further vascularized to fabricate 3D prevascularized constructs for full thickness skin wound repair [8,9]. Importantly, to meet the stringent standard for engineering or biomanufacturing functional 3D tissues, the hMSC sheet needs to be complete and highly uniform.

To obtain a complete cell sheet, including the hMSC sheet, cells have been seeded on a transferable surface other than the regular cell culture treated plastic, in order to minimize the damage to cells, ECM structure, as well as the cell-ECM connection caused by cell detachment [10]. The thermoresponsive surface approach is well accepted because it allows for cell detachment without external force via shifting of the surface wettability at certain temperatures [11]. However, the fabrication process was cost-intensive and facility-dependent. In addition, the thermoresponsive surface needs to be grafted with cell adhesive molecules to ensure cell attachment [12]. Considering the high cost of materials and efforts for the long-term culture of cell sheet, it is crucial to develop an economical and stable substrate surface for easily harvesting intact cell sheets.

Polydimethylsiloxane (PDMS) has been employed in biological applications as an inert, stable and biocompatible material. Nevertheless, PDMS is hydrophobic and has poor cell adhesion. Plasma etching followed by collagen adsorption is the conventional method for converting PDMS from hydrophobic to hydrophilic to enhance cell adhesion. The collagen was accumulated on the surface via weak forces such as electrostatic, hydrophobic, and van der

* Corresponding author.
E-mail address: fengzhao@mtu.edu (F. Zhao).
Peer review under responsibility of KeAi Communications Co., Ltd.

https://doi.org/10.1016/j.bioactmat.2018.01.005

Waals. Therefore, it is fairly easy for the collagen molecules to leach into the solution, resulting in a non-uniform collagen coating [13]. We have found in our previous research that this could eventually lead to a patchy cell sheet, which severely impedes its application for biomanufacturing functional 3D completely biological tissues.

Layer-by-layer grafting of (3-aminopropyl)triethoxy silane (APTES), glutaraldehyde, and collagen I has been developed to covalently bind collagen on the PDMS surface for enhancing cell adhesion and proliferation [14]. In this study, we further demonstrated that the covalent grafting method significantly improved the collagen distribution on PDMS surface, which led to higher hMSC sheet formation efficiency and lower defect rate for long-term hMSC sheet culture. By utilizing this low-cost method, uniform hMSC sheets could be fabricated, allowing massive cell sheet production to fulfill the demand of for completely biological tissue engineering and biomanufacturing applications.

2. Materials and Methods

2.1. Layer-by layer grafting on PDMS

PDMS substrate was prepared from a SYLGARD 184 Silicone Elastomer Kit (Dow-corning, Midland MI) under manufacturer's instruction. The mixture was poured into a mold, degassed, and cured at 65 °C for 4 h to achieve a homogenous sheet. The PDMS sheets were then punched into 20 mm diameter disks. These PDMS disks were cleaned and dried overnight before being plasma etched for 60 s (radio frequency (RF) power 100 W, chamber pressure 200 mTor, O_2). Treated disks were grafted with the first layer of 10% (3-Aminopropyl)triethoxysilane (APTES, Sigma-Aldrich, St Louis, MO) in ethanol for 2 h followed by two ethanol rinses. The second layer of 2.5% Glutaraldehyde (GA, Sigma-Aldrich) in deionized water was grafted for 1 h followed by two washes in deionized water. Both grafted and non-grafted disks were sterilized under ethanol and UV light for one hour. Sterilized disks were immersed in a collagen I solution (20 μg/mL, Sigma-Aldrich) for 2 h at room temperature. These samples were split up into four groups including plain PDMS control (C), plasma etching only (P), non-grafted (adsorption), and layer-by-layer grafted (grafting) groups.

2.2. Chemical composition characterization

Fourier Transform Infrared Spectroscopy (FTIR) was applied to record the chemical composition of the samples with attenuated total reflectance (ATR) mode. Spectra of pristine PDMS, plasma treated PDMS, plasma treated PDMS with 2 h collagen adsorption were tested to investigate their surface changes in adsorption groups. The pristine PDMS, plasma treated PDMS, APTES modified PDMS, GA coated PDMS after APTES modification and collagen grafted PDMS by layer and layer coating were also tested respectively to compare their surface changes after each grafting step. The samples were fresh made and air dried before test. The spectra were recorded at room temperature in the 700–3700 cm^{-1} range by using a FTIR-ATR spectrometer (Perkin-Elmer, Waltham, MA).

2.3. Surface wettability characterization

Each surface treatment group was evaluated using the static sessile drop method in order to determine the contact angle that water droplets make with the surface. Each treatment group was tested on multiple samples, and in multiple locations on each sample using G10 contact angle measurement system (Krüss, Germany). Deionized water was used to form pendant droplets.

2.4. Surface morphology analysis by atomic force microscopy (AFM)

The surface morphology of all PDMS substrates were characterized by AFM, which was carried out with a Dimension ICON AFM system (Bruker, Billerica, MA). Tapping mode was applied to map the substrate surfaces. Average deviation was evaluated by the cantilever, and considered as surface roughness.

2.5. Cell culture

Bone marrow derived hMSCs were obtained from Texas A&M University Health Sciences Center. Passage 4 hMSCs were seeded on PDMS substrate surfaces at an initial density of 10,000 cells/cm^2. The samples were cultured in complete α-minimum essential medium (α-MEM) containing 20% FBS, 1% glutamine, and 1%penicillin/streptomycin (Thermo Fisher Scientific, Waltham, MA) for up to 14 days with medium changes every 72 h.

2.6. Fluorescent imaging

Samples were obtained after the cell culture and fixed in 3.7% formaldehyde solution (J.T.Baker, Center Valley, PA) for 30 min. Rhodamine phalloidin (Invitrogen, Carlsbad, CA) was used to label actin filaments within hMSCs. Briefly, the cells were blocked with 1% bovine serum albumin (Thermo Fisher Scientific) and incubated with rhodamine phalloidin (1:200 v/v) for 1 h. The cell sheet thickness after 14 days culture was measured by Z-stack scanning using Olympus FV-1000 confocal microscopy. Cell area was derived from these images using ImageJ particle analysis. To do this, the particle size was adjusted to exclude non-cell components, and the contained areas of each image's binary thresholds were measured in order to obtain the final cell area values.

2.7. DNA assay

The DNA content in the samples was determined fluorometrically using PicoGreen assay kit (Life Technologies). Briefly, cells were lysed using proteinase K solution (Sigma-Aldrich) at 37 °C. 100 μL lysed sample from each group was placed in triplicate in a 96-well plate and mixed with 100 μL of Picogreen working solution (Thermo Fisher Scientific), followed by 10 min dark incubation at room temperature. The incubated plate was read by a Fluoroskan Ascent FL fluorescent plate reader (Thermo Fisher Scientific).

2.8. Quantitative reverse transcription polymerase chain reaction (qRT-PCR)

RNA isolation was performed on samples using the RNeasy Mini Kit (Qiagen, Valencia, CA), followed by cDNA synthesis via a reverse transcription kit (Life Technologies, Rockville, MD). The gene expression of cell binding integrins α_2 and β_1 as well as the stemness genes OCT-4 and SOX-2 were analyzed. KiCqStart® SYBR® Green Primers (Sigma-Alderich) were used and the genes analyzed were integrinα_2 gene ITGA-2 (Forward: 5′-GGTGGGGTTAATTCAGTATG; Reverse: 5′-ATATTGGGATGTCTGGGATG), integrin β_1 gene ITGB1(Forward: 5′-ATTCCCTTTCCTCAGAAGTC; Reverse: 5′-TTTTCTTCCATTTTCCCCTG), OCT-4 (Forward: 5′-GATCACCCTGGGATATACAC; Reverse: 5′-GCTTTGCATATCTCCTGAAG), and SOX-2 (Forward: 5′-ATAATAACAATCATCGGCGG; Reverse: 5′-AAAAAGAGAGGCAAACTG). A one step plus system (Applied Bioscience, Waltham, MA) was used for qPCR cycles. Acquired gene expression data of grafting samples was normalized to adsorption samples, and folding difference was obtained by the ΔΔCt method.

2.9. Statistical analysis

Results from each experiment were triplicated, and presented as means ± standard deviation. The T-test function of Excel (Microsoft, Redmond, WA) was used for comparisons between groups, and statistical significance was accepted at $p < 0.05$.

3. Results

3.1. Collagen coating efficiency, surface wettability, and roughness

As shown by Fig. 1a, the PDMS was treated by oxygen plasma to oxidize its surface for effective APTES binding. GA was then employed as a crosslinking agent between APTES and collagen I molecules. This resulted in covalent binding of collagen I to the PDMS surface. Immunofluorescent staining of collagen I showed improved uniformity of the collagen coating on grafting samples (Fig. 1b). The wettability of control, plasma treated, adsorption, and grafting surfaces was examined by the contact angle measurements. The control surfaces had the highest average contact angle at $102.25 \pm 3.4°$. Plasma treatment caused the contact angle decrease to $32.33 \pm 5.9°$, which was the lowest of all the surfaces. The adsorption surface had a contact angle of $66.77 \pm 3.6°$, which increased to $85.61 \pm 4.4°$ for the covalent bonding surface as seen in Fig. 2a and b.

The surface coating was further characterized by FTIR spectra (Fig. 3), in which the transformation at around 1255, 1014, 793 cm^{-1} indicated the Si-CH_3, Si-O-Si, Si-CH_3 stretching in PDMS

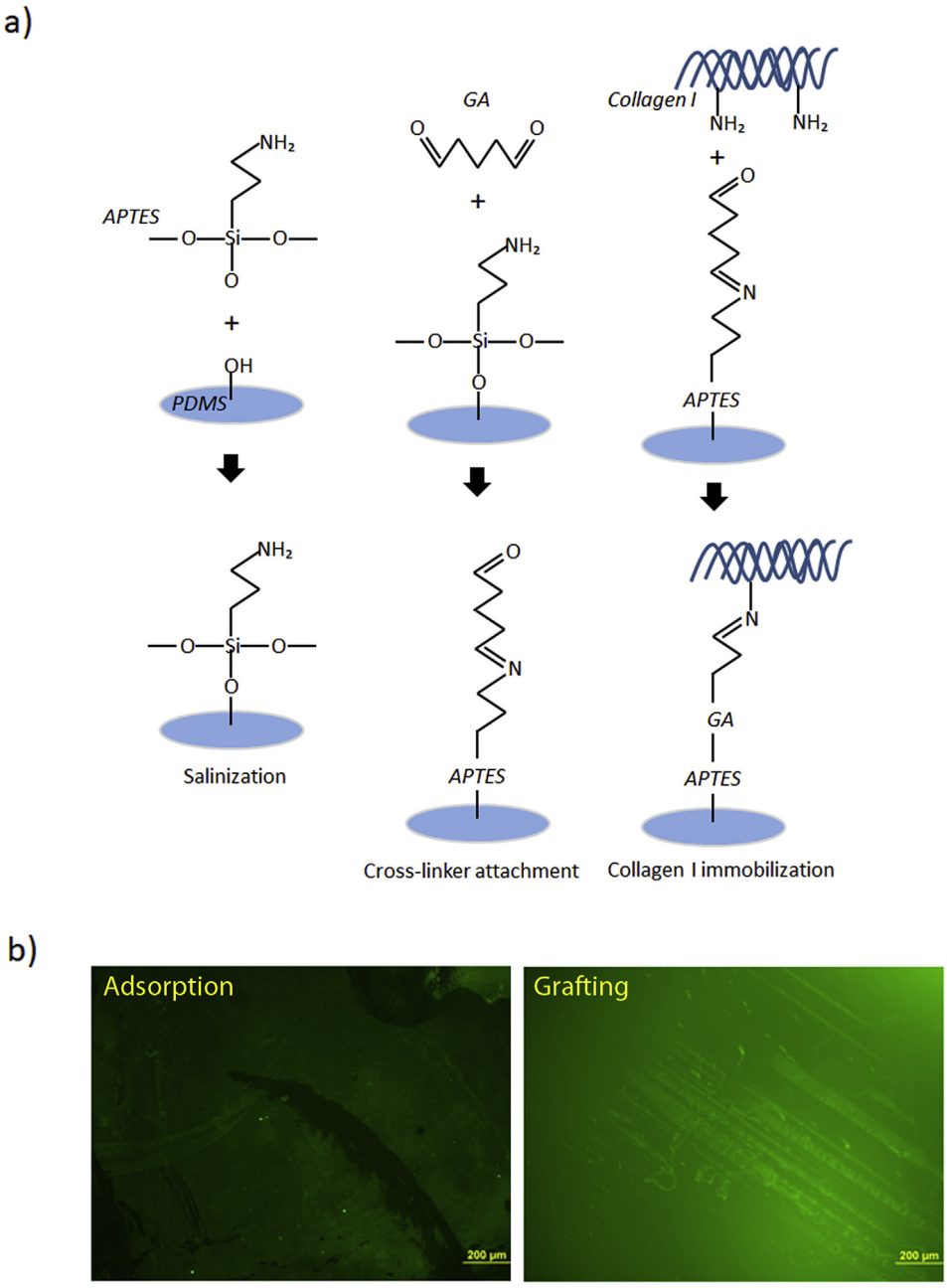

Fig. 1. Layer-by-layer collagen I grafting on PDMS surfaces. a) Schematic diagram of Layer-by-layer collagen I grafting chemistry. b) Collagen I fluorescent intensity on adsorption and grafting surfaces. The grafting surface had more and uniform collagen I fluorescent intensity and more uniformity than the adsorption surface.

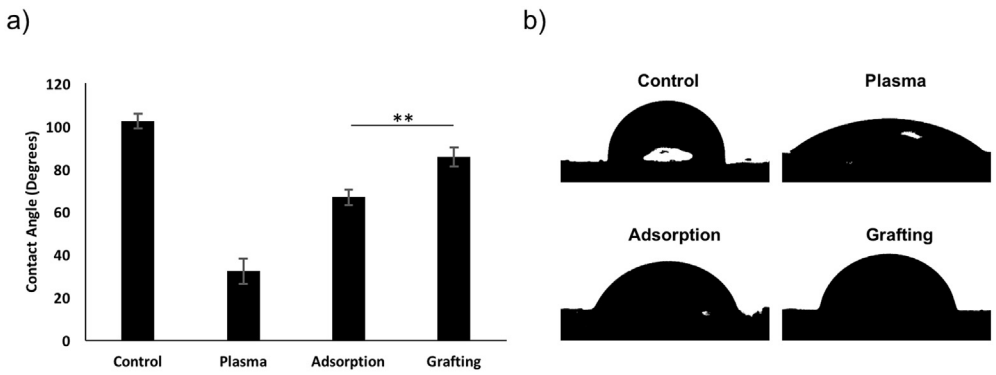

Fig. 2. Wettability of different prepared PDMS surfaces. a) Quantification of contact angle measurement. The higher contact angle on the grafting surface indicated that there was more collagen present on this sample. b) Representative water droplet formation on different surfaces. (**$p < 0.01$).

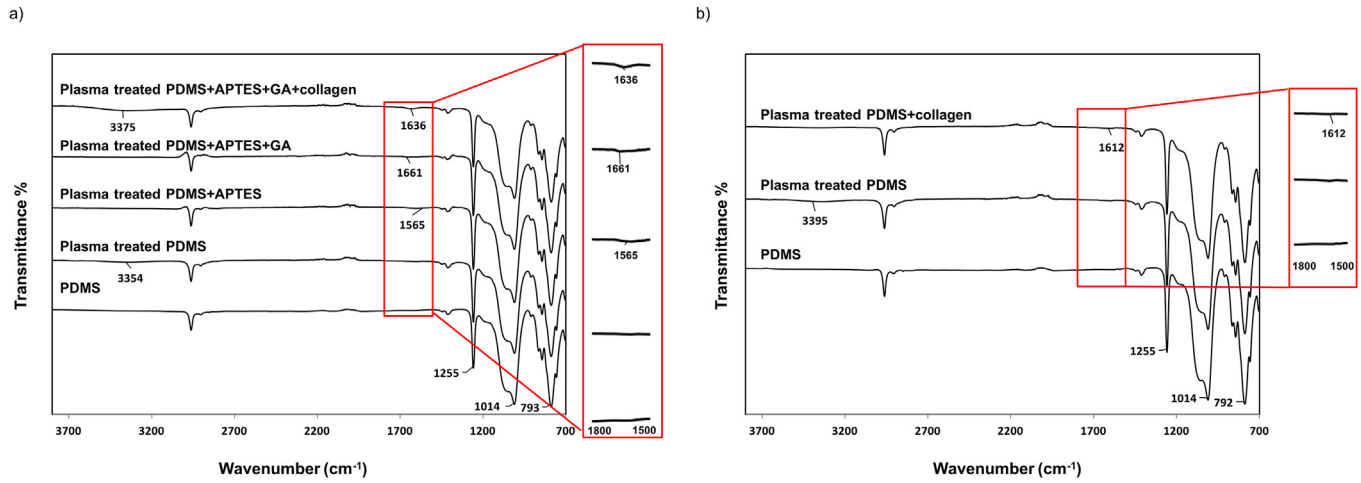

Fig. 3. FTIR-ATR spectra of grafting group (a) and adsorption group (b) in the range of 3700–700 cm^{-1}. The peaks of interest have been emphasized by numerical values. The grafting method resulted in detectable signal after collagen coating while the adsorption method did not generate obvious collagen signal.

[15]. As shown in Fig. 3a, after plasma treatment, a broad peak appeared around 3354 cm^{-1}, demonstrating the presence of O-H stretching after O_2 plasma [16]. Next, after the APTES conjugation, there was a new small broad peak around 1565 cm^{-1}, which was attributed to the formation of aminebicarbonate salt ($-HN_3(HCO_3)^-$) [17]. There was also a small peak appeared at around 1661 cm^{-1} after the GA grafting, indicating the vibration of C=N after APETS and GA reaction [18]. Finally, after the collagen grafting, the collagen functional groups emerged around 3375 and 1636 cm^{-1} due to the association of O-H and N-H stretching in collagen, as it has been proven that the amide indication could be observed around 3350, 1700–1600 cm^{-1} [19,20]. While in the adsorption group (Fig. 3b), there were only a few negligible transformations, such as the deformation of spectra around 1612 cm^{-1}, which was resulted from the absorbed collagen. Overall, the FTIR results indicated that covalent bonds formed between collagen and PDMS via the grafting method. Compared with the adsorption method, the grafting method incorporated more collagen on the PDMS surface.

The surface morphologies of control, adsorption, and grafting samples were mapped over a 400 μm^2 area by AFM. Both surface morphologies and their respective roughness were shown in Fig. 4. The control sample had a relatively smooth surface (0.68 ± 0.04 μm) in comparison to the collagen-coated groups (adsorption, grafting), with grafting showing the highest roughness (11.95 ± 1.34 μm, $p < 0.01$), and adsorption between the two (4.74 ± 0.13 μm).

3.2. Cell sheet formation

hMSCs were seeded on adsorption and grafting surfaces to allow for cell sheet formation. At 6 h, cells on the grafting surface were more evenly spread than adsorption surface. At day 3, cell spread and coverage were similar on both surfaces. At day 7, a monolayer of cells had formed on adsorption surfaces; however, defects were observed on some of the adsorption surfaces (Fig. 5a). The grafting surfaces had lower cell density but fewer defects were detected. At day 14, large voids were found on most adsorption surfaces, while homogenous cell sheets were maintained on the grafting surfaces. Analysis of these images using ImageJ showed that there was more cell coverage on adsorption surfaces on day 7, but coverage significantly dropped at day 14 (Fig. 5b and c). In comparison, the total cell area on grafting surfaces steadily increased throughout the entire culture period. At day 14, a uniform hMSC layer was formed on the grafting PDMS while the cell layer on the adsorption PDMS shrank to a patchy structure. Complete cell sheets from grafting groups could be easily detached from the PDMS substrate while largely maintaining their original shape (Fig. 5d). The average thickness and average shrinkage ratio of hMSC sheets in grafting groups was 36.86 ± 4.35 μm and 17.5 ± 2.8%, respectively.

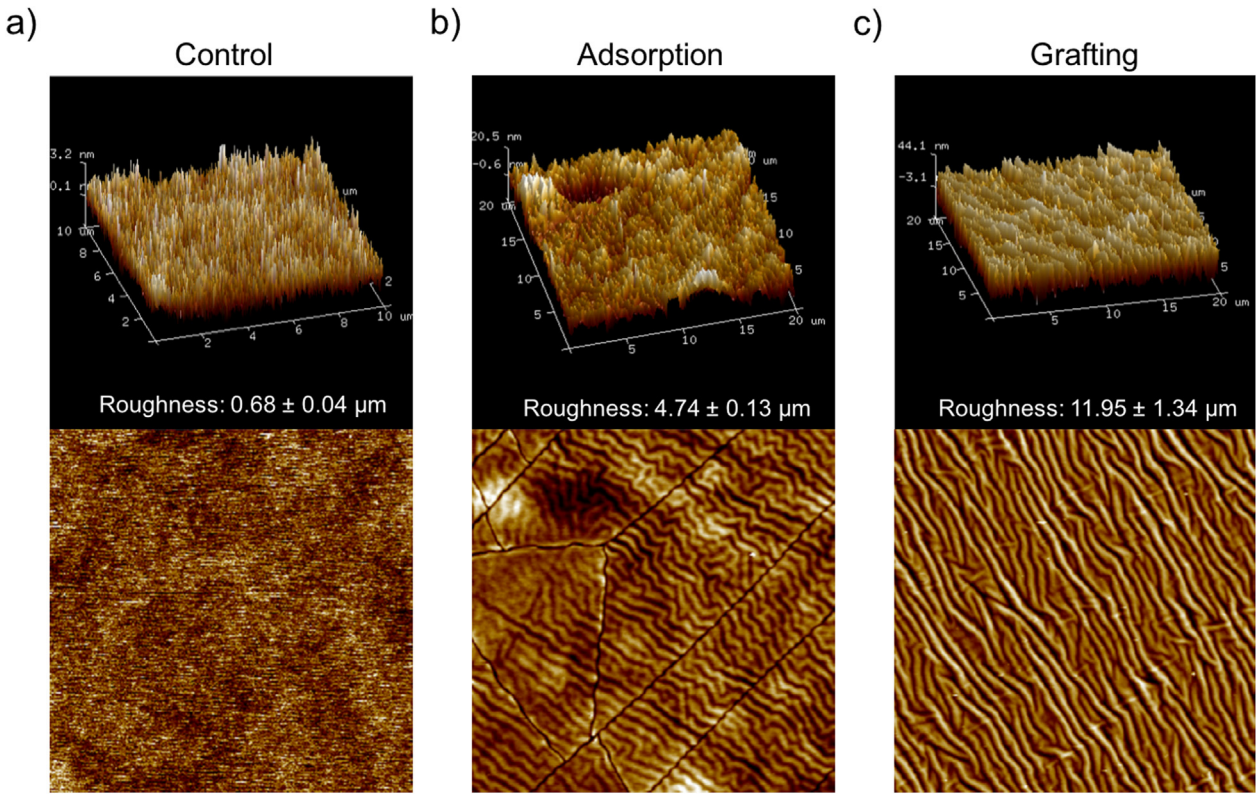

Fig. 4. Representative surface morphology and roughness of PDMS control (a), adsorption surface (b), and grafting surface (c) mapped by AFM. The grafting surface showed a more uniform coating.

3.3. Gene expression of cell sheets

mRNA was extracted from the harvested cell sheets, and analyzed for cell adhesion integrin complex $\alpha_2\beta_1$ from both grafting and adsorption surfaces. The integrin α_2 (15 folds) and β_1 (25 folds) gene expression in grafting samples was dramatically higher than adsorption samples at day 7. The folding difference dropped at day 14, but both integrin α_2 and β_1 gene expression were still higher in the grafting samples (Fig. 6a).

The stemness gene expression was also investigated. Compared to adsorption surfaces, grafting samples showed increased OCT-4 but decreased SOX-2 expression from day 2 to day 14. Most fold expressions were close to 1, which demonstrated that both samples had comparable stemness (Fig. 6b).

4. Discussion

To develop a cost efficient and less equipment dependent bioactive surface for stable and long-term hMSC sheet engineering, the collagen I grafting technology was investigated through layer-by-layer chemistry. The PDMS was plasma treated to provide an oxidized surface for APTES to bind. GA was then employed as a crosslinking agent between APTES and collagen I molecules. A thorough study from Yang et al., has reported that the current, power and duration of plasma oxidation significantly affects the topography of PDMS substrates [21]. Based on our contact angle measurements, the plasma treatment conditions we used changed the PDMS surface to hydrophilic, indicating the retention of hydroxyl groups. The layer-by-layer grafting also significantly increased the roughness of the PDMS surface, suggesting more collagen was covalently bound to the PDMS. Compared to the direct adsorption of collagen I onto PDMS, a more stable and homogeneous coating was produced on the grafted PDMS surface (Figs. 1 and 3).

Cells bind to specific motifs in collagens such as RGD peptides, through integrin receptors [22]. Adsorption of collagen I on substrate surface for cell culture was simple and affordable, thus it was used as “an universal” method to enhance cell adhesion and survival for different cell and surface types [23,24]. This method was relying on the adsorption of collagen I onto the polymer surface via weak interactions [13]. Nevertheless, the deposited layer through adsorption was not an ideal host for long-term cell sheet culture. As observed, cells tend to detach due to the contractile force produced by cell-cell interaction once the confluent layer was formed. This phenomenon could potentially happen due to the time-lapse loss of the adsorbed collagen I layer under cell culture medium and cell homeostasis. Potential reasons include the heterogeneity of the collagen I layer as a result of adsorption when collagen I molecule adsorbed on the PDMS surface. Moreover, the adsorbed collagen I could be replaced by other proteins contained in the cell culture medium via Vroman effect. In this case, the adsorbed collagen was replaced by other proteins in the serum, which led to the loss of cell adhesion binding sites [25,26]. Additionally, the pH of the culture medium steadily decreased as a result of cell metabolism [27]. The decreasing pH in the medium could result in depletion of adsorbed collagen I from any uncovered PDMS surface, as similar stability loss was found in bovine serum albumin (BSA) adsorption [28]. Consequently, as observed in Fig. 4a, the cell adhesion of the adsorption samples was prohibited in those collagen binding diminished sites, which resulted in cell-absent areas at day 7 and day 14. In this situation, actin fiber-dense boundaries were observed around the void spaces, while total cell number was not affected (Fig. 4b). In contrast, the layer-by-layer grafting method eliminated the weak interaction between collagen I and PDMS by

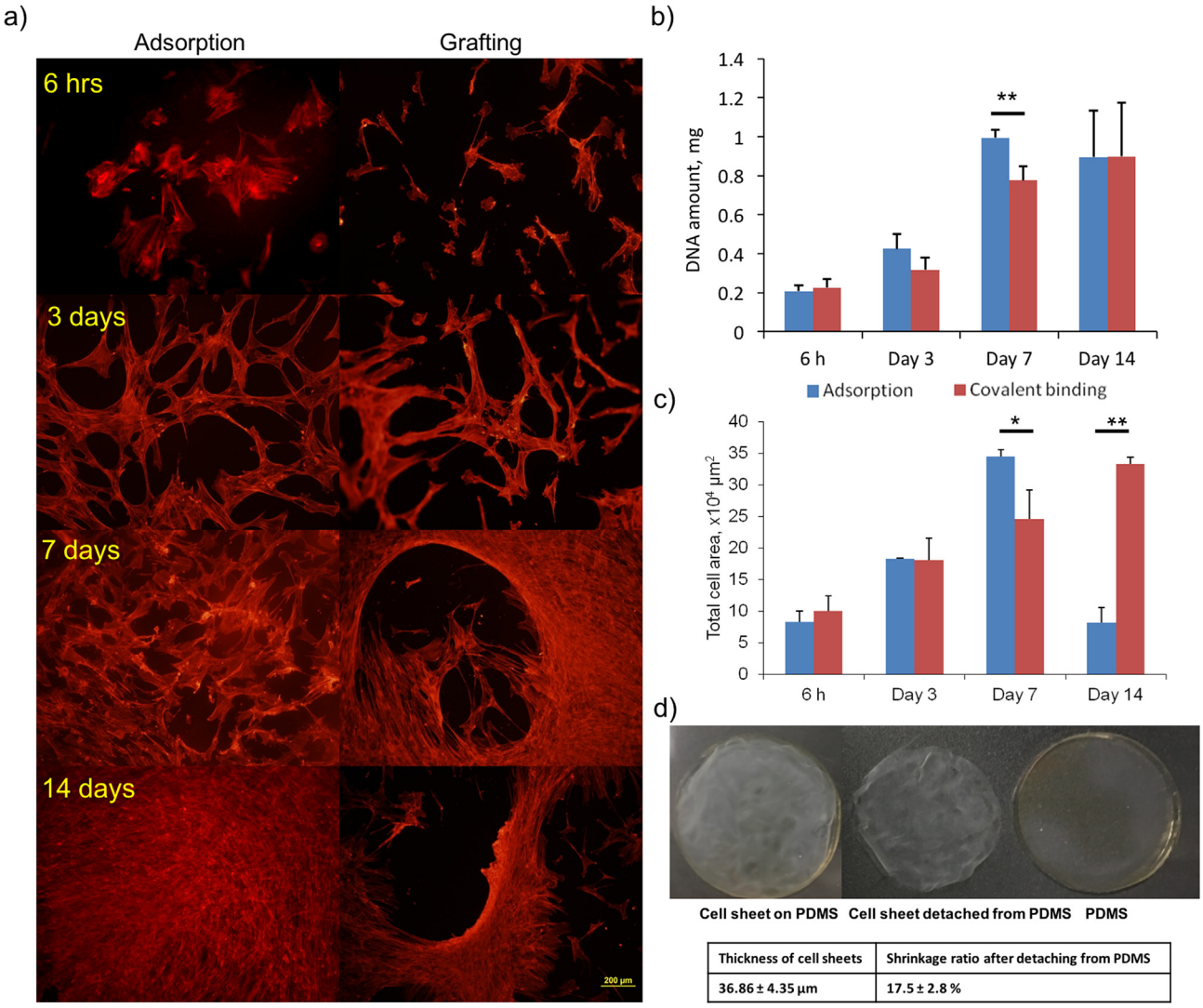

Thickness of cell sheets	Shrinkage ratio after detaching from PDMS
36.86 ± 4.35 μm	17.5 ± 2.8 %

Fig. 5. hMSC sheet formation on different surfaces over 14 days: F-actin filament of MSCs (a), DNA quantification (b), total cell cover area (c), and cell sheet morphology (d). (*$p < 0.05$, **$p < 0.01$). A uniform and complete cell sheet was generated from the grafting surface after the 14-day culture.

the APTES-GA spacing, while providing covalent binding between collagen I and -NH2 functional groups, thus produced a homogenous collagen I coating (Fig. 1). The full coverage of collagen I also provided cell adhesion binding sites to promote even growth of the cell sheets (Fig. 5a).

Surface wettability and roughness affects cell adhesion, proliferation, and migration [29]. We performed wettability assessment to verify the hydrophobic collagen I coating layer (Fig. 2). However, it was proved that wettability was not a critical factor for hMSCs adhesion on modified PDMS surface [30]. Research has also shown that cell adhesion potential increased with roughness, but the cell motility was decreased [31]. In this study, we observed that the rougher collagen I grafting surface (Fig. 4c) had lower total cell area coverage until day 14 (Fig. 5a), while hMSC adhesion was not diminished in comparison with adsorption surfaces (Fig. 5a and c). Higher surface roughness also indicated that more collagen I molecules were grafted onto the surface compared to the adsorption samples. After 14 days culture, complete cell sheets with an average thickness 36.86 ± 4.35 μm were detached from PDMS substrates in grafting groups, while no complete cell sheet could be obtained from adsorption groups. The cell sheets well maintained their uniformity and original shape, which would facilitate their future applications for 3D tissue biofabrication.

Integrin complex $\alpha_2\beta_1$ are transmembrane proteins that bind cells to type I collagen (collagen I) [26]. They also play roles of mediating cell spreading and migration [32]. We have found a significant up-regulation of integrin $\alpha_2\beta_1$ gene expression in hMSCs grown on the collagen grafting surfaces compared with those on adsorption groups at day 7 (Fig. 6a), suggesting that more integrin $\alpha_2\beta_1$ mediated focal adhesion sites were generated. The increased cell-surface binding sites facilitated cell attachment and prevented the cells from detachment. This observation was critical for improving the success rate of long-term cell sheet culturing. In addition, compared with the adsorption samples, the stem cell nature of the cell sheet was not affected by the process. Stem cell genes OCT-4 and SOX-2 represents the stemness of hMSCs [33]. The OCT-4 and SOX-2 gene expression results showed no significant difference between adsorption and grafting groups (Fig. 6b), suggesting that the layer-by-layer grafting treated PDMS surface did not significantly alter the stemness of hMSCs. The results proved the feasibility of the layer-by-layer grafting strategy for stem cell sheet culture, which provided better cell sheet morphology while maintaining the undifferentiated status of hMSCs.

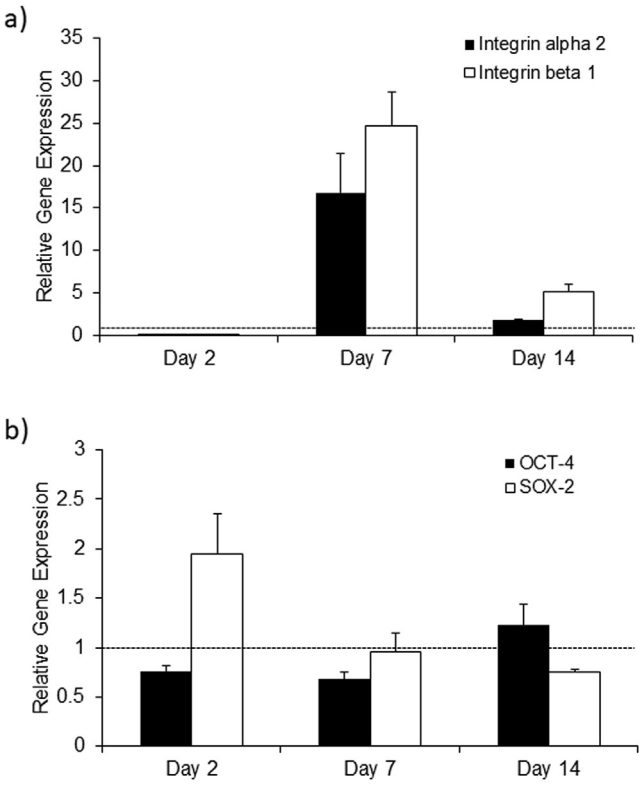

Fig. 6. The adhesion molecule (a) and stemness (b) gene expression of hMSCs cultured on grafting surfaces as compared to adsorption surfaces. The integrin α_2 and β_1 gene expression in grafting samples was significantly higher than adsorption samples from day 7, whereas the stemness gene expression was comparable in the two types of samples over the 14 day culture period. (Dash line: folding difference = 1).

5. Conclusions

We have demonstrated an enhanced collagen I-grafted surface for stable and cost effective long-term hMSC sheet engineering. The layer-by-layer grafting through APTES and GA resulted in a homogenous collagen I layer, which improved the cell adhesion and attachment through enhanced roughness and reliable collagen I binding sites. Moreover, the stemness of hMSCs were not affected by this cell sheet generation strategy. This method could potentially benefit the mass production of long-term cell sheets to fulfill the tissue engineering and biomanufacturing demands.

Acknowledgements

This study was supported by the National Institutes of Health (1R15CA202656) and the National Science Foundation (1703570).

References

[1] F.J. O'Brien, Biomaterials & scaffolds for tissue engineering, Mater. Today 14 (3) (2011) 88–95.
[2] G.D. DuRaine, et al., Emergence of scaffold-free approaches for tissue engineering musculoskeletal cartilages, Ann. Biomed. Eng. 43 (3) (2015) 543–554.
[3] M.A. Nandkumar, et al., Two-dimensional cell sheet manipulation of heterotypically co-cultured lung cells utilizing temperature-responsive culture dishes results in long-term maintenance of differentiated epithelial cell functions, Biomaterials 23 (4) (2002) 1121–1130.
[4] K. Sakaguchi, T. Shimizu, T. Okano, Construction of three-dimensional vascularized cardiac tissue with cell sheet engineering, J. Contr. Release 205 (Supplement C) (2015) 83–88.
[5] Q. Xing, et al., Natural extracellular matrix for cellular and tissue biomanufacturing, ACS Biomater. Sci. Eng. 3 (8) (2017) 1462–1476.
[6] R. Hass, et al., Different populations and sources of human mesenchymal stem cells (MSC): a comparison of adult and neonatal tissue-derived MSC, Cell Commun. Signal. CCS 9 (2011), 12–12.
[7] B. Parekkadan, J.M. Milwid, Mesenchymal stem cells as therapeutics, Annu. Rev. Biomed. Eng. 12 (12) (2010) 87–117.
[8] L. Zhang, et al., Hypoxia created human mesenchymal stem cell sheet for prevascularized 3D tissue construction, Adv. Healthc. Mater. 5 (3) (2016) 342–352.
[9] L. Chen, et al., Pre-vascularization enhances therapeutic effects of human mesenchymal stem cell sheets in full thickness skin wound repair, Theranostics 7 (1) (2017) 117–131.
[10] I. Elloumi-Hannachi, M. Yamato, T. Okano, Cell sheet engineering: a unique nanotechnology for scaffold-free tissue reconstruction with clinical applications in regenerative medicine, J. Intern. Med. 267 (1) (2010) 54–70.
[11] Y. Kumashiro, et al., Modulation of cell adhesion and detachment on thermoresponsive polymeric surfaces through the observation of surface dynamics, Colloids Surfaces B Biointerfaces 106 (Supplement C) (2013) 198–207.
[12] M.T. Moran, et al., Intact endothelial cell sheet harvesting from thermoresponsive surfaces coated with cell adhesion promoters, J. R. Soc. Interface 4 (17) (2007) 1151–1157.
[13] S.E. Woodcock, W.C. Johnson, Z. Chen, Collagen adsorption and structure on polymer surfaces observed by atomic force microscopy, J. Colloid Interface Sci. 292 (1) (2005) 99–107.
[14] S. Kuddannaya, et al., Surface chemical modification of poly(dimethylsiloxane) for the enhanced adhesion and proliferation of mesenchymal stem cells, ACS Appl. Mater. Interfaces 5 (19) (2013) 9777–9784.
[15] L.M. Johnson, et al., Elastomeric microparticles for acoustic mediated bioseparations, J. Nanobiotechnol. 11 (1) (2013) 22.
[16] D.B.T. Mascagni, et al., Corrosion resistance of 2024 aluminum alloy coated with plasma deposited aC: H: Si: O films, Mater. Res. 17 (6) (2014) 1449–1465.
[17] E.F. Vansant, P. Van Der Voort, K.C. Vrancken, Preface, Elsevier, 1995.
[18] D. Zhang, et al., Immobilization of cellulase on a silica gel substrate modified using a 3-APTES self-assembled monolayer, SpringerPlus 5 (1) (2016) 48.
[19] B. de Campos Vidal, M.L.S. Mello, Collagen type I amide I band infrared spectroscopy, Micron 42 (3) (2011) 283–289.
[20] J. Leivo, et al., A durable and biocompatible ascorbic acid-based covalent coating method of polydimethylsiloxane for dynamic cell culture, J. R. Soc. Interface 14 (132) (2017), 20170318.
[21] Y. Yang, et al., Effects of topographical and mechanical property alterations induced by oxygen plasma modification on stem cell behavior, ACS Nano 6 (10) (2012) 8591–8598.
[22] J. Heino, The collagen family members as cell adhesion proteins, BioEssays 29 (10) (2007) 1001–1010.
[23] K.Y. Chumbimuni-Torres, et al., Adsorption of proteins to thin-films of PDMS and its effect on the adhesion of human endothelial cells, RSC Adv. 1 (4) (2011) 706–714.
[24] J. Witos, et al., Collagen I and III and their decorin modified surfaces studied by atomic force microscopy and the elucidation of their affinity toward positive apolipoprotein B-100 residue by quartz crystal microbalance, Analyst 136 (18) (2011) 3777–3782.
[25] K.A. Heyries, C.A. Marquette, L.J. Blum, Straightforward protein immobilization on sylgard 184 PDMS microarray surface, Langmuir 23 (8) (2007) 4523–4527.
[26] J. Jokinen, et al., Integrin-mediated cell adhesion to type I collagen fibrils, J. Biol. Chem. 279 (30) (2004) 31956–31963.
[27] M. Naciri, D. Kuystermans, M. Al-Rubeai, Monitoring pH and dissolved oxygen in mammalian cell culture using optical sensors, Cytotechnology 57 (3) (2008) 245–250.
[28] S. Ghosh, H.B. Bull, Adsorbed films of bovine serum albumin: tensions at air-water surfaces and paraffin-water interfaces, Biochim. Biophys. Acta 66 (Supplement C) (1963) 150–157.
[29] Y. Arima, H. Iwata, Effect of wettability and surface functional groups on protein adsorption and cell adhesion using well-defined mixed self-assembled monolayers, Biomaterials 28 (20) (2007) 3074–3082.
[30] J.M. Curran, R. Chen, J.A. Hunt, The guidance of human mesenchymal stem cell differentiation in vitro by controlled modifications to the cell substrate, Biomaterials 27 (27) (2006) 4783–4793.
[31] M. Lampin, et al., Correlation between substratum roughness and wettability, cell adhesion, and cell migration, J. Biomed. Mater. Res. 36 (1) (1997) 99–108.
[32] J. Jokinen, et al., Integrin-mediated cell adhesion to type I collagen fibrils, J. Biol. Chem. 279 (30) (2004) 31956–31963.
[33] R. Izadpanah, et al., Biologic properties of mesenchymal stem cells derived from bone marrow and adipose tissue, J. Cell. Biochem. 99 (5) (2006) 1285–1297.